Research Article

Guanghai Liu*, Ming Gao, Changjiang Liu, Yusheng Xu, Xiongxing Zhang, and Haibin Chen

High-speed multi-spectral explosion temperature measurement using golden-section accelerated Pearson correlation algorithm

https://doi.org/10.1515/phys-2025-0138
received November 19, 2024; accepted March 07, 2025

Abstract: To measure transient and extremely high temperatures of explosion processes, a high-speed multi-spectral temperature measurement system was developed. By measuring spectral radiant exitance corresponding to six wavelengths by six fast photodetectors, transient explosion temperature can be extracted in realtime through a linear correlation algorithm accelerated by the golden-section method. Real explosion experiments with the energetic material polymer-bonded explosive demonstrated that the method could rapidly and accurately determine explosion temperatures. Peak explosion temperature up to 3,560 K has been successfully extracted. The proposed method may find applications in explosive evaluations.

Keywords: multi-spectral pyrometer, emissivity, golden-section method, explosion, temperature measurement

1 Introduction

Temperature is an important parameter for industrial manufacture, chemical synthesis, agriculture, and so on [1–7]. In military and civil engineering applications, to evaluate the performance of explosives, explosion experiments are usually conducted, in which, explosion temperature, is also one of the most important parameters for evaluation. Explosion temperature greatly affects performances of explosives in demolition, mining, or defense systems. However, because of the violent, destructive, and rapidly changing characteristics of the explosion process, temperature measurements are generally extremely challenging.

Explosion temperature measurements are conducted using two types of methods, *i.e.*, contact and noncontact methods. Thermocouples [8] and fiber optical probes [9] have been proposed for the direct measurement of high temperatures in explosive fireballs, with capabilities to measure high temperatures exceeding 1,900 K. However, these devices are limited by poor repeatability and a relatively low upper limit for the measurement range. Moreover, as direct contact is necessary for heat transfer, the response speed is too low for transient high temperature measurements. Furthermore, these sensors lacked the robustness needed to withstand the extreme conditions of explosive fireballs.

In comparison to the contact method, without using the slow heat transfer mechanism, and the sensing part does not need direct withstand extremely high temperature, noncontact approaches can more accurately and quickly obtain the transient temperature, and the upper measurement limit can be considerably expanded to much higher temperature value. The most widely used noncontact method is radiation thermometry, which determines the temperature of a surface or volume by measuring the emitted electromagnetic radiation [10–13]. Various types of radiation pyrometers have been developed, including two color pyrometers [14,15], multiwavelength pyrometers [16–19], and polarization pyrometers [20,21]. Multiwavelength pyrometers are widely used because they can obtain accurate temperatures over a large measurement range by effectively overcoming the influence of varying emissivity on the measured results. The multiwavelength pyrometer samples spectral radiant exitance at several different wavelengths (more than two) and determines the temperature by fitting through radiation curve of a standard blackbody source. The most widely used technique is the emissivity construction method proposed by Gebbie *et al.* and Svet [22,23], in which an assumed model of spectral emissivity is considered, and the least

*** Corresponding author: Guanghai Liu**, School of Optoelectronic Engineering, Xi'an Technological University, Xi'an 710021, Shaanxi, China; National Key Laboratory of Energetic Materials, Xi'an 710018, Shaanxi, China; Sichuan Physcience Optics and Fine Mechanics Co., Ltd, 621000, Mian Yang, Sichuan, China, e-mail: guanghailiu@163.com
Ming Gao, Changjiang Liu, Yusheng Xu, Xiongxing Zhang, Haibin Chen: School of Optoelectronic Engineering, Xi'an Technological University, Xi'an 710021, Shaanxi, China

squares method is commonly used for temperature calculation [24,25]. However, this method is limited owing to the lack of *a priori* knowledge of spectral emissivity. In many cases, a simple assumed emissivity model can result in a relatively large uncertainty in the calculated temperature. Particularly for temperature measurements in explosion processes, accurate determination of the spectral emissivity consistent with the actual case is rather difficult, as a result, the fast and accurate estimation of temperature is challenging.

To solve the aforementioned problem, in this study, we built a fast response six wavelength fiber-type multi-spectral pyrometer, and inspired by new development of numerical and semi-analytical methods [26–28], we proposed a Pearson correlation algorithm accelerated by the golden-section method for high-speed temperature extraction without using the emissivity model. By directly calibrating the measurement system to a blackbody source, the explosion temperature measurement result can be more accurate. With the usage of the golden-section acceleration, the extracting efficiency of the temperature extraction can be greatly improved to satisfy the realtime high-speed output requirement. We performed simulations and experiments, which demonstrated that the temperature change process is consistent with actual results; the uncertainty of the calculated temperature could also be effectively reduced.

2 Methods

2.1 Multi-spectral explosion temperature measurement principle

All objects above absolute zero continuously emit thermal radiation. The thermal radiation has a specific spectral distribution, and the amount of thermal radiation at a specific wavelength depends only on the temperature of the object and is not related to any other properties, which renders noncontact temperature acquisition through radiation measurement possible.

The radiation characteristics of a thermally radiating object can be described by a quantity called the spectral radiant exitance, *i.e.*, the radiation flux per unit wavelength interval emitted per unit area from the surface of the thermally radiating object. The spectral radiant exitance is related to temperature and has a certain distribution form in the wavelength domain. For most cases, the blackbody radiation model can be used, the spectral radiation exitance can be given by Planck's law [11]:

$$M(\lambda, T) = \frac{c_1}{\lambda^5} \cdot \frac{1}{e^{\frac{c_2}{\lambda T}} - 1}, \tag{1}$$

where $c_1 = 3.7418 \times 10^{-16}$ W/m^2, $c_2 = 1.4388 \times 10^{-5}$ K, M is the spectral radiant exitance, λ is the wavelength, and T is the temperature.

From Eq. (1), the spectral radiant exitance corresponds to the temperature at a specific wavelength. The maximum of the spectral radiant exitance gradually shifts to the shorter wavelength with the increase in temperature, and the spectral radiant exitance distribution only depends on the temperature, so if the distribution in wavelength domain can be obtained, the temperature can be extracted accordingly, which constitutes the theoretical foundation of radiation thermometry.

For this purpose, an optical spectrum analyzer may be the best choice. However, optical spectrum analyzers generally operate at a relatively low speed, which cannot satisfy fast temperature measurement requirements of explosion tests. In an actual fast measurement of explosion temperature, several optical filters with specific wavelengths are used to separately filter out radiation at different wavelengths, and several photodetectors with fast response times are used to simultaneously monitor the filtered radiation. This is the basic concept in which multi-spectral radiation thermometry is grounded.

When photodetectors with optical filters are used as measurement devices in the linear working region, the relationships between output voltages of photodetectors and spectral radiant exitance at different wavelengths can be expressed as

$$M_{0i} = K_i V_i / \Delta\lambda_i, \quad i = 1, 2, 3, \ldots, N, \tag{2}$$

where λ_i is the wavelength of the ith measurement channel, and K_i is the calibration coefficient of the ith channel, which needs to be predetermined before temperature measurements; V_i is the output voltage of the ith channel obtained from the corresponding photodetector; $\Delta\lambda_i$ is the bandwidth of the ith measurement channel; and N is the total number of monitored wavelength channels. The spectral radiant exitances M_{0i} at each channel can be obtained based on the calibration coefficient K_i, output voltage V_i, and bandwidth $\Delta\lambda_i$ at each channel. The calibration coefficients K_i generally have some uncertainties, which will result in errors in each monochromatic radiant exitances of M_i, and finally affect the accuracy of the temperature measurement. However, in our case, the temperature is extracted through a correlation method, the monochromatic radiant exitances of M_i are all

viewed as random variables with some errors, the calculation method has very strong robustness. With the increase in errors in M_i, the correlation coefficient may deviate from the ideal value of 1; however, the maximum can still work well for temperature extraction.

Using a well-designed calculation algorithm, the temperature T of the explosion fireball can be determined by determining the best matching curve of blackbody radiance. The matching degree of the measured data with the spectral radiant exitance curve of a blackbody with temperature T can be evaluated using the Pearson correlation coefficient [29]

$$R_{MM_0}(T_j) = \frac{\sum_{i=1}^{n}(M_{0i} - \overline{M_0})(M(\lambda_i, T_j) - \overline{M(\lambda_i, T_j)})}{\left\{\sum_{i=1}^{n}(M_{0i} - \overline{M_0})^2 \sum_{j=1}^{n}(M(\lambda_i, T_j) - \overline{M(\lambda_i, T_j)})^2\right\}^{\frac{1}{2}}}, \quad (3)$$

where $R_{MM_0}(T_j)$ is the Pearson correlation coefficient of the radiant exitances between the measured explosion fireball and blackbody at temperature T_j. M_{0i} is the measured spectral radiant exitance of the ith wavelength channel, and $M(\lambda_i, T_j)$ is the calculated spectral radiant exitance from Eq. (1) with the ith wavelength λ_i under the jth temperature T_j.

From our actual temperature measurements and calculations, the relationship between the correlation coefficient and temperature is a simple curve with only one maximum (Figure 1). The maximum temperature corresponds to the actual temperature. Thus, different temperatures were tested in a specific range. The actual temperature of the object could be determined by comparing the correlation coefficients and searching for the maximum value.

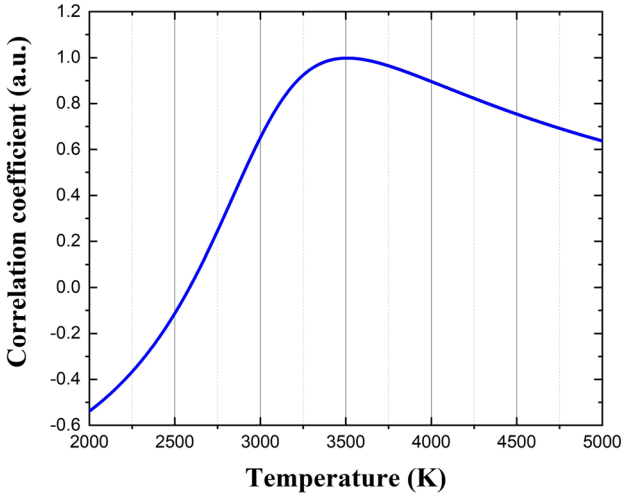

Figure 1: Relationship between correlation coefficient and temperature.

2.2 Temperature extraction by golden-section accelerated Pearson correlation algorithm

To guarantee the maximum value of the correlation coefficient, according to the empirical value of the maximum explosion temperature of the explosives, a temperature of 2,000–5,000 K can be used as the temperature seeking range. If the temperature resolution is set to 1 K, 3,001 one by one calculations are required. Evidently, the number of calculations is too large, and the time required to obtain the temperature is relatively long. Several different searching algorithms have been considered, such as binary search, gradient descent, and golden-section algorithms. The binary search is proper for the searching of a result in a monotonic sequence. In our case, the relationship between the correlation coefficient and the temperature is not monotonic, so the binary search is not suitable. The gradient descent algorithm is generally suitable for the peak searching of functions or sequences with multiple variables. For cases with a single variable, whether with a fixed or variable searching step, multiple rounds of searching are needed. The efficiency cannot be guaranteed for the fast extraction of temperature. In comparison, the golden-section algorithm [30] is simple, direct, and efficient; thus, we introduce the golden-section algorithm for the maximum correlation coefficient search to significantly reduce the amount of computation.

To extract the temperature of the measured object, an algorithm based on the Pearson correlation with the golden-section algorithm was proposed. The flowchart is shown in Figure 2, and the program flow is described below.

Step 1: We obtain the output voltage V_i at all wavelength channels and calculate the spectral radiant exitance M_i using Eq. (2) at these channels.

Step 2: We set the lower and upper values T_L and T_U of the temperature searching range (where the lower temperature value is 2,000 K and the upper temperature value is 5,000 K), and $T'_L = T_L + 0.382(T_U - T_L)$ and $T'_U = T_L + 0.618(T_U - T_L)$ as the first two lower and upper testing values of the measured temperature. The two numbers 0.618 and 0.382 come from the gold-section ratio, *i.e.*, $(\sqrt{5} - 1)/2 \approx 0.618$, and $0.382 = 1–0.618$.

Step 3: Using Eq. (1), we calculate the spectral radiant exitance corresponding to the wavelength channels of the measurement system at these two temperatures, and determine the correlation coefficients for these two temperatures using Eq. (3).

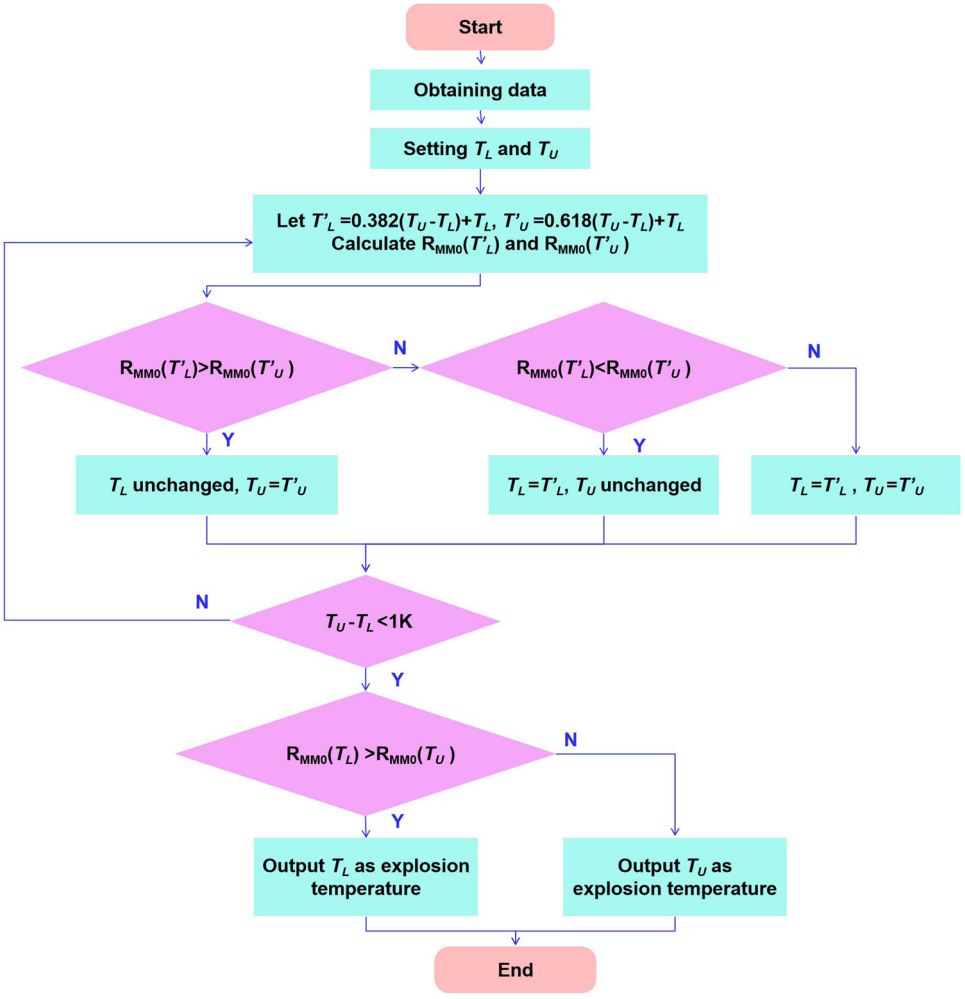

Figure 2: Flowchart of golden-section accelerated Pearson correlation algorithm.

Step 4: If $R_{MM_0}(T'_L) > R_{MM_0}(T'_U)$, we let $T_U = T'_U$ and keep T_L unchanged; if $R_{MM_0}(T'_L) < R_{MM_0}(T'_U)$, we let $T_L = T'_L$ and keep T_U unchanged. If $R_{MM_0}(T'_L) = R_{MM_0}(T'_U)$, we let $T_L = T'_L$ and $T_U = T'_U$.

Step 5: We repeat Steps 3 and 4 with the updated parameters until the searching range is smaller than 1 K. Subsequently, we compare the correlation coefficients at T_U and T_L, where the temperature with a larger correlation coefficient is determined as the measured temperature of the object.

According to the golden-section algorithm, for the temperature range of 2,000–5,000 K, at most 18 calculations can yield the final result, which significantly increases the efficiency of explosion temperature extraction.

3 Explosion temperature simulation

After explosive denotation, an explosion fireball will be generated that will expand outward rapidly. Theoretically, describing the entire fireball expansion and the temperature distribution changing process will be relatively difficult because of the complicated fluid and chemical reaction dynamic processes. However, the temperature at the initial stage of the firewall can be estimated relatively accurately by simulation.

In the initial stage of fireball expansion, the main characteristic of an explosion is outward expansion of the explosion products. To approximate the real state of the explosion products, ideal gas equation is inadequate. The fireball temperature can be calculated using the wellknown

semiempirical Becker–Kistiakowski–Wilson (BKW) state equation, which viewed the explosion products as a very dense gas. The BKW state equation [31] is given in the following equation:

$$\frac{pV_m}{RT} = 1 + \kappa \sum x_i k_i [V_m(T + \theta)^{\alpha}] e^{\beta\kappa \sum x_i k_i [V_m(T+\theta)^{\alpha}]}, \quad (4)$$

where p is the pressure, V_m is the molar volume of the explosion products, R is the ideal gas constant, and T is the thermodynamic temperature of the explosion products; κ, α, β, and θ are all empirical constants, and k_i and x_i are the covolume and molar fraction of the ith material, respectively. In the calculation, the radiation loss is negelected, because the corresponding heat loss rate is far lower than the internal energy conversion rate.

For the polymer-bonded explosive (PBX) used in the experimental test, the explosion and BKW parameters were calculated using the thermochemical software EXPLO5 (Tables 1 and 2). In the initial expansion stage, the temperature of the explosion products decreased from the temperature of the Chapman-Jouguet (CJ) state to a specific value. For the PBX, the temperature of the CJ state, *i.e.*, the explosion temperature, was calculated to be 3559.90 K; when the explosion product expanded to the initial density, the corresponding temperature was 2,700 K.

From the simulation results in Figure 3, before the explosion fireball reaches the measurement point, the temperature of the measurement point is the same as that of the environment; when the explosion fireball reaches the monitoring point, the temperature rapidly increases to a peak of 3558.90 K. With further outward expansion of the explosion fireball, the temperature of the measured point decreases to the initial value.

To characterize the surface temperature of the explosion fireball, we set a group of measurement points to obtain the peak temperatures at these points, which could be used to obtain the equivalent temperature variation in the fireball surface. The surface temperature gradually decreases with the outward expansion of the explosion fireball (Figure 4). Within 0.02 ms, the surface temperature reduces from a peak temperature of 3,500 K to a temperature of 2,700 K. The quick decrease in the peak temperature come from the quick change in the pressure and specific volume caused by the fast outward expansion of the explosion fireball.

Table 2: Calculated BKW parameters

α	β	θ	κ
0.5	1.86	34.81	0.8846

4 Experiments

4.1 Multi-spectral explosion temperature measurement system

The multi-spectral temperature measurement system comprises an optical probe, a long transmission fiber, a 1 × 6 optical coupler, six optical filters and photodetectors, a data acquisition system, and a computer (Figure 5).

The optical probe was in the form of a multi-mode fiber protected by a stainless steel tube, which pointed to the measured position of the object. The long transmission fiber (Shenzhen Optical Communication Co. Ltd, multimode silica fiber with wide passing band, core diameter: 600 μm, NA = 0.37) was used to transmit back the thermal radiation collected by the optical probe. The thermal radiation was then split into six parts using a 1 × 6 optical coupler (Shenzhen Optical Communication Co. Ltd, FSMA905-1-6). The six parts of the radiation were coupled into free space at the six output facets. After passing through six optical filters with different narrow passing bands, the thermal radiation was focused onto the photosensitive surfaces of the six fast photodetectors (Guilin Guangyi Intelligent Technology Co. Ltd, PD12A-100M and PD12C-100M). The six optical filters (Shanghai Mega-9 Optoelectronic Co., Ltd, BP532/20K, BP700/20K, BP825/20K, BP1310/20K, BP1450/20K, BP1650/20K) were all narrowband filters with a passing bandwidth of approximately 20 nm, and their center wavelengths were 0.532, 0.7, 0.825, 1.31, 1.45, and 1.65 μm, respectively. The wavelengths were selected to cover both sides of the peak spectral radiation

Table 1: Typical parameter values of explosive

Energetic material	Density (g/cm^3)	CJ pressure (Mbar)	Detonation velocity (cm/s)	Explosion heat (MJ/kg)	Constant volume specific heat (MJ/kg/K)
PBX-MY	1.86	34.81	0.8846	0.108	0.792

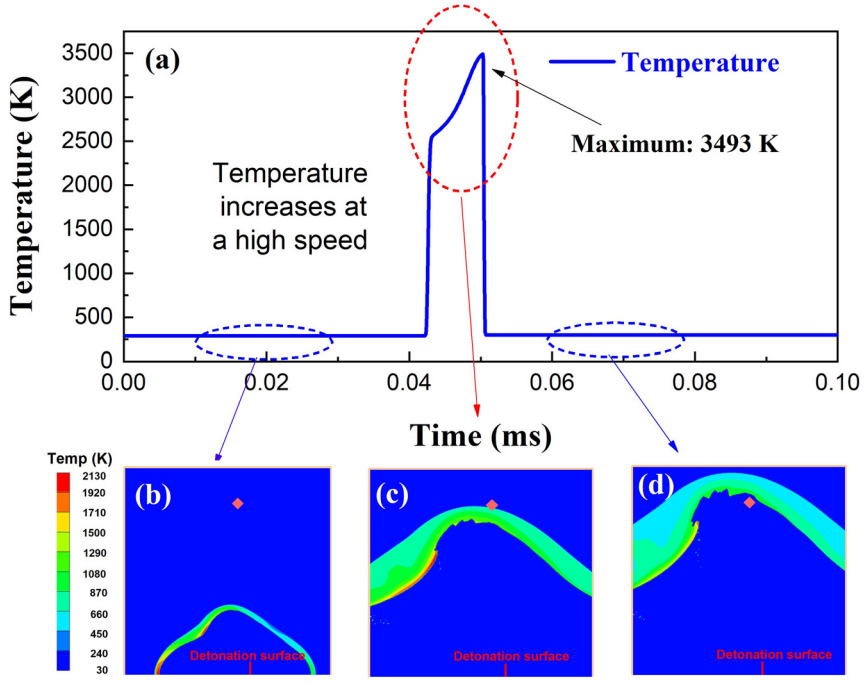

Figure 3: Simulated temperature change at a monitoring point in time domain. (a) Temperature distributions before (b), when (c), and after (d) the fireball surface is arriving.

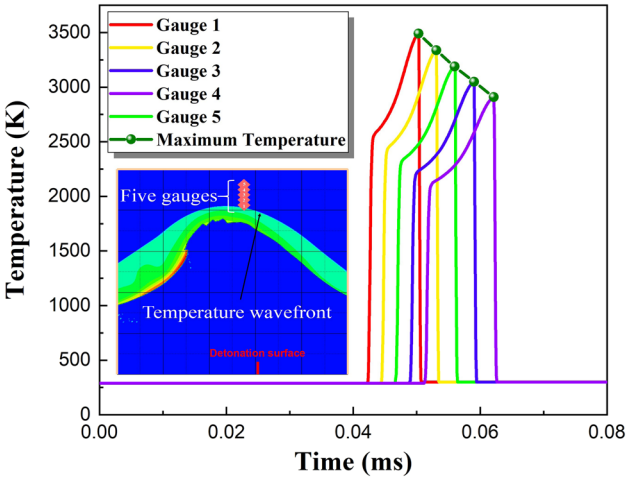

Figure 4: Simulated temperature change in firewall surface in time domain.

exitance on the radiation curve when the measured object is with a high temperature of 2,000–4,000 K, which is suitable for the high temperature measurement of explosion process.

The thermal radiation was then converted into electric voltage signals by the six photodetectors. For the three optical channels with wavelengths of 0.532, 0.7, and 0.825 μm, silicon detectors were used. For the other three channels of 1.31, 1.45, and 1.65 μm, InGaAs detectors were used. The response time of these photodetectors was 10 ns, which satisfied the requirement for transient temperature measurements in explosion processes. The voltage outputs from the six photodetectors were then collected by the data acquisition system (Beijing Yixin Tech. Co. Ltd, M4i-4451 × 8, six channel bandwidths: 100 MHz, sampling rate: 500 MSa/s), and transmitted to the computer for temperature calculation using a software program based on the golden-section accelerated Pearson correlation method. The response time of the photodetectors and the bandwidth and sampling rate of the data acquisition system could also satisfy the fast temperature measurement requirement of the transient explosion process.

4.2 System calibration

A 24 V 150 W quartz halogen tungsten lamp as a blackbody source was used to calibrate the radiation temperature measurement system. The optical probe was fixed and pointed to the quartz halogen tungsten lamp at a distance of about 3 m, which is the same distance between the optical probe and the explosive in explosion temperature measurement. The relationship between the temperature and driving current/voltage of the tungsten lamp was previously calibrated by the China Institute of Testing Technology. The calibration results are listed in Table 3.

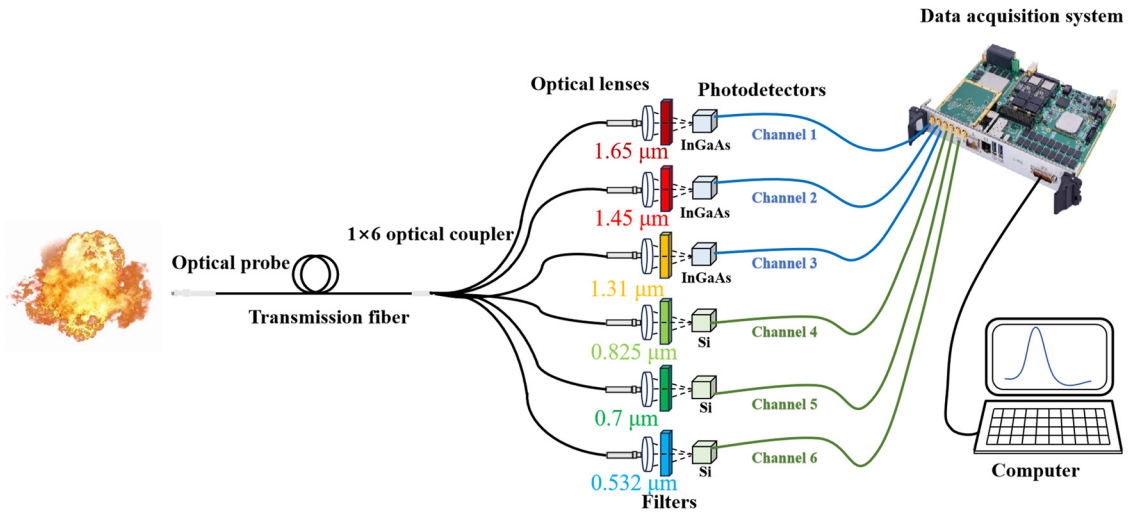

Figure 5: Schematic of multi-spectral temperature measurement system.

At a driving current of 5.12 A, the corresponding temperature T_C is 2,600 K. The halogen tungsten lamp operated smoothly 30 min after turning on and was used to calibrate the multi-spectral temperature measurement system. The output voltages for all wavelength channels are listed in Table 4. Using Eq. (2) and considering the output voltages of the six wavelength channels, the calibration coefficients K_i can be determined, as listed in Table 4. With these calibration coefficients, the spectral radiant exitances at the six wavelength channels can be calculated using Eq. (2); using the correlation coefficients given by Eq. (3), the explosion temperature can be obtained.

4.3 Explosion temperature measurement

A photograph of the explosion test site is presented in Figure 6. The explosion experiment was conducted in an open field without any buildings. A section of a 100 m long silica optical fiber with a wide transmission band was used to transmit the thermal radiation collected by the optical probe near the explosion center back to the main temperature measurement system in a safe testing room, which was a small shelter that can shield any explosion products. The optical fibers were sealed in a corrugated stainless steel tube to prevent damage from the explosion. The measured data were obtained quickly and recorded using this system. The energetic material was remote detonated electrically after confirming security.

The energetic material used was a PBX, which consisted of 95% octogen, 4.3% fluorouracil as a binder, and 0.7% graphite as a desensitizing agent. The density was approximately 1.86 g/cm^3. The explosive was cylindrical with a diameter of 25 mm and a height of 60 mm. It was placed on an explosive carrier with the optical probe fixed on a pillar at a distance of 3 m from the explosive. The optical probe was placed at the same height as the explosive cylinder and pointed toward its center.

4.4 Experimental results and analysis

A system with a golden-section accelerated Pearson correlation algorithm was used to obtain the explosion

Table 3: Characteristic parameters of halogen tungsten lamp

Current (A)	Voltage (V)	Temperature (K)
3.52	7.74	2,042
3.95	9.54	2,200
4.52	12.16	2,400
5.12	15.23	2,600
5.93	19.86	2,856
6.41	22.84	3,000

Table 4: Output voltages and calibration coefficients at six wavelengths channels with T_c = 2,600 K

Wavelength (μm)	Output voltage (mV)	Calibration coefficient (10^{-6}, W/V/nm)
0.532	205.6	1.70126
0.70	356.3	1.06891
0.825	645.87	1.36348
1.31	783.91	1.50392
1.45	435.8	1.12508
1.65	693.8	2.03005

Figure 6: Photograph of explosion test site.

temperature from the real explosion experiments. The PBX explosion experiments were conducted under the same condition for two times. The variation curves of the output voltages of the six wavelength channels in the time domain were recorded (Figure 7). The optoelectronic signals from all six wavelength channels changed in a microsecond time scale, so the response time of the photodetectors, and the bandwidth, sampling rate of the data acquisition system are fast enough for the quick extraction of the radiation temperature. It can be observed that the detailed transient output voltages of the six channels are different for the two times of measurement. Because the explosion of explosives is a drastic dynamic process accompanied by violent chemical reactions and physical changes, detailed transient process will be very different for each time. The results

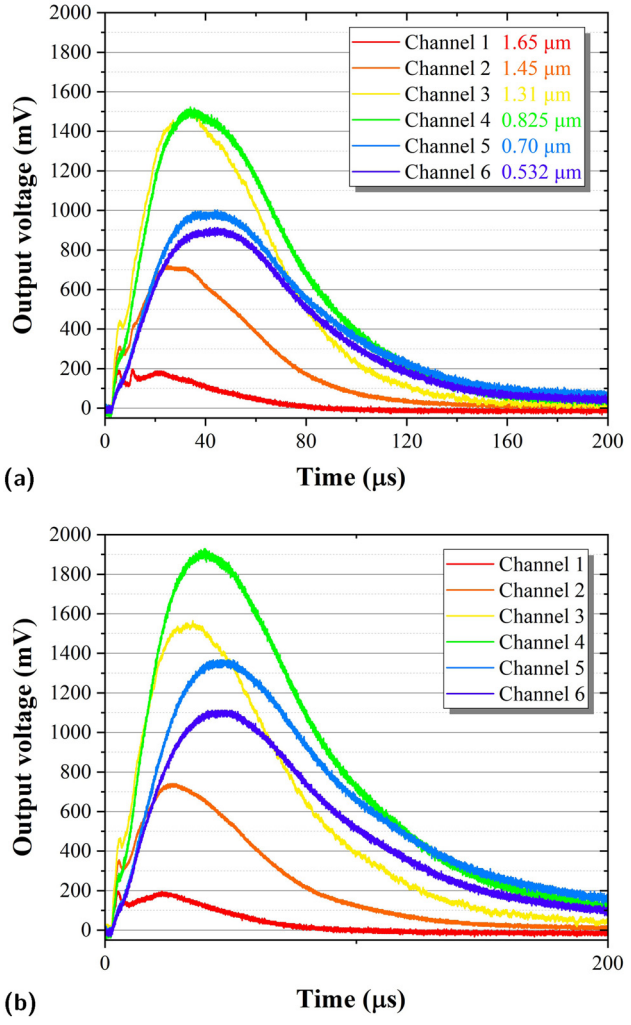

Figure 7: Output voltages at six wavelength channels in time domain. (a) First explosion and (b) second explosion.

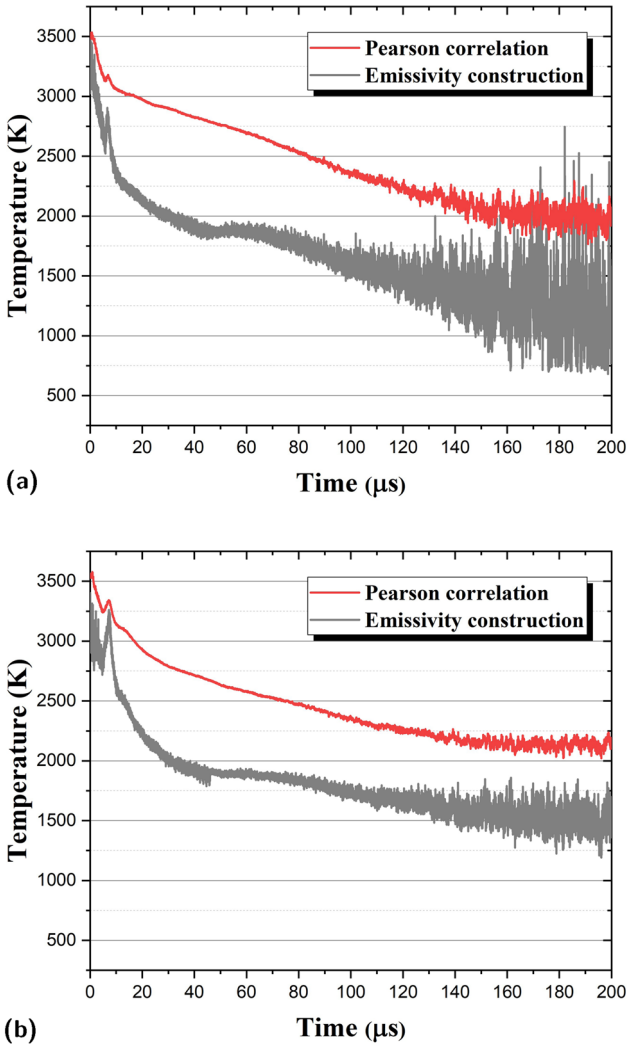

Figure 8: Temperature change with time of the two explosion processes obtained by the Pearson correlation and emissivity construction algorithms. (a) First explosion and (b) second explosion.

show that the temperature measurement system can correctly respond to the spectral radiant exitances in each wavelength channel.

The temperatures obtained for the two explosions were calculated based on the experimental data. The temperature change curves are shown in Figure 8. Two calculation methods were used in this study. One was based on the emissivity construction method, and the other was based on the Pearson correlation method. The output of the photodetectors gradually increased to their peaks in a time scale of several tens of microsecond. However, the temperature increased to their peak values in a much short time duration, maybe, a few nanoseconds. It should be noted that the temperature extracted is directly related to the relative light intensities received by the photodetectors but not their absolute values. In our case, limited by the sensitivities and response times of our measurement system, this initial temperature increasing process was failed to be distinguished. We will try to solve the problem in our further study by improving the measurement system by using better photodetectors and faster data acquisition system.

From the results shown in Figure 8, the maximum temperatures extracted for the two explosions using the Pearson correlation method are 3,501 and 3,560 K, respectively, and the maximum temperatures extracted using the emissivity construction method are 3,400 and 3,420 K, respectively. The results extracted from the proposed method were closer to the simulated results, of 3,500 K. The reason for the large deviation of the emissivity construction method may come from the uncertainty of the emissivity, which quickly changes in the explosion process and can hardly be given precisely. It can also be noted that the peak temperatures extracted for the two cases have a difference of 59 K, which is normal, because the explosion of explosives is a rapid, violent chaotic process accompanied by generations of large amount of heat and gases, and the detailed process cannot be the same for each case. Furthermore, the uncertainty in the temperature results extracted using the emissivity construction method was considerably larger. In comparison, the uncertainty in the temperature results obtained using the Pearson correlation method was considerably lower. Thus, the proposed Pearson correlation method performed better than the emissivity construction method for explosion temperature measurements.

5 Conclusion

In conclusion, for radiation temperature measurement of explosive explosion, we developed a high-speed fiber-type six-wavelength multi-spectral pyrometer and proposed a golden-section accelerated Pearson correlation method for the fast temperature extraction. After calibrating the temperature measurement system with a halogen tungsten lamp, rapid explosion temperature changes in explosion experiment of PBX, were successfully extracted. Highest temperature of up to 3,560 K was successfully obtained. In comparison with the results of the emissivity construction method, our extracted temperatures were more consistent with the simulation and experimental results, and the temperature calculation uncertainty was effectively reduced. The rapid temperature increasing process was failed to be extracted in our study, which will be focused to resolve by improving the sensitivity and bandwidth of the measurement system. The proposed method may find applications in explosive evaluations.

Funding information: The research was supported by the Key R&D Plan of Shaanxi Province, China, Grant No. 2024GX-YBXM-041, and National Key Laboratory of Energetic Materials, China, Grant No. 2024-XXXX-XX-JJ-046-06.

Author contributions: Conceptualization: G.L.; methodology: M.G.; software: C.L.; validation: G.L. and X.Z.; Resources: H.C.; data curation: C.L.; writing – original draft Preparation: G.L.; writing – review and editing: M.G.; and funding acquisition: H.C. All authors have accepted responsibility for the entire content of this manuscript and approved its submission.

Conflict of interest: The authors state no conflict of interest.

Data availability statement: The datasets generated and/or analysed during the current study are available from the corresponding author on reasonable request.

References

[1] Abbas IA. Generalized thermoelastic interaction in functional graded material with fractional order three-phase lag heat transfer. J Cent South Univ. 2015;22:1606–13.
[2] Abbas IA, Saeed T, Alhothuali M. Hyperbolic two-temperature photo-thermal interaction in a semiconductor medium with a cylindrical cavity. Silicon 2020;13:1871–8.
[3] Alzahrani FS, Abbas IA. Photo-thermal interactions in a semiconducting media with a spherical cavity under hyperbolic two-temperature model. Mathematics. 2020;8(4):585.
[4] Carrera E, Abouelregal AE, Abbas IA, Zenkour AM. Vibrational analysis for an axially moving microbeam with two temper-atures. J Therm Stresses. 2015;38(6):569–90.
[5] Abbas IA, Othman MIA. Plane waves in generalized thermo-microstretch elastic solid with thermal relaxation using finite element method. Int J Thermophys 2012;33:2407–23.

[6] Malik MF, Shah SAA, Bilal M, Hussien M, Mahmood I, Akgul A, et al. New insights into the dynamics of heat and mass transfer in a hybrid (Ag-TiO2) nanofluid using modified Buongiorno model: a case of a rotating disk. Results Phys. 2023;53:106909.
[7] Mladenoviç ZZ, Gocić S.. Effect of electron temperature and concentration on production of hydroxyl radical and nitric oxide in atmospheric pressure low-temperature helium plasma jet: Swarm analysis and global model investigation. Open Phys. 2024;22(1):20240055.
[8] Frost DL, Clemenson J, Goroshin S, Zhang F, Soo M. Thermocouple temperature measurements in metalized explosive fireballs. Prop Explos Pyrotech. 2021;46(6):899–911.
[9] Lebel LS, Brousseau P, Erhardt L, Andrews WS. Measurements of the temperature inside an explosive fireball. J Appl Mech. 2013;80(3):031702.
[10] Tischler M. High accuracy temperature and uncertainty calculation in radiation pyrometry. Metrologia. 1981;17(2):49–57.
[11] DeWitt DP, Nutter GD. Theory and practice of radiation thermometry. New York, USA: John Wiley & Sons;1991.
[12] Xin CS, Dai JM, Wang YL. Development of optical fiber twenty-spectral radiation pyrometer. Infra Technol. 2008;30(1):47–50.
[13] Fu T, Liu J, Duan M, Zong A. Temperature measurements using multicolor pyrometry in thermal radiation heating environments. Rev. Sci. Instrum. 2014;85(4):044901.
[14] Anselmi-Tamburini U, Campari G, Spinolo G, Lupotto P. A two-color spatial-scanning pyrometer for the determination of temperature profiles in combustion synthesis reactions. Rev Sci Instrum. 1995;66(10):5006–14.
[15] Müller B, Renz U. Development of a fast fiber-optic two-color pyrometer for the temperature measurement of surfaces with varying emissivities. Rev Sci Instrum. 2001;72(8):3366–74.
[16] Kosonocky WF, Kaplinsky MB, Mccaffrey NJ, Edwin SHH, Constantine NM, Nuggehalli MR, et al. Multiwavelength imaging pyrometer. Proc. SPIE: Infrared Detectors and Focal Plane Arrays III; 1994 July 15. Orlando, FL, United States; 1994.
[17] Lyzenga GA, Ahrens TJ. Multiwavelength optical pyrometer for shock compression experiments. Rev Sci Instrum. 1979;50(11):1421–4.
[18] Duvaut T, Georgeault D, Beaudoin JL. Multiwavelength infrared pyrometry: optimization and computer simulations. Infrared Phys Technol. 1995;36(7):1089–103.
[19] Krapez JC. Measurements without contact in heat transfer: multiwavelength radiation thermometry. Principle, implementation and pitfalls, Thermal measurements and inverse techniques. San Francisco: Taylor & Francis; 2019.
[20] Ni PA, More RM, Yoneda H, Bieniosek FM. Polarization pyrometry: An improvement to multi-wavelength optical pyrometry. Rev Sci Instrum. 2012;83(12):123501.
[21] Svet DY, Sayapina VI. Effect of polarization on the accuracy of optical pyrometers. Meas Tech. 1970;13(2):235–8.
[22] Gebbie HA, Bohlander RA, Futrelle RP. Properties of photons determined by interferometric spectroscopy. Nature 1972;240(5381):391–4.
[23] Svet DI. Determination of the emissivity of a substance from the spectrum of its thermal radiation and optimal methods of optical pyrometry. European Conference on Thermophysical Properties of Solids at High Temperatures, 5th; High Temperatures, High Pressures; 1976 May 18–21. Moscow, USSR; 1976.
[24] Coates PB. The least-squares approach to multi-wavelength pyrometry. High Temp High Pressures. 1988;20(4):433–41.
[25] Hoch M. Multiwavelength pyrometry: radiance temperature versus wavelength curve should be used for temperature determination. Rev Sci Instrum. 1992;63(9):4205–7.
[26] Haider JA, Ahmad S, Ghazwani HA, Hussien M, Almusawa MY, Az-Zo'Bi EA. Results validation by using finite volume method for the blood flow with magnetohydrodynamics and hybrid nanofluids. Mod Phys Lett B. 2024;38(24):2450208.
[27] Khan SA, Yasmin S, Waqas H, Az-Zo'Bi EA, Alhushaybari A, Akgület A, et al. Entropy optimized Ferro-copper/blood based nanofluid flow between double stretchable disks: application to brain dynamic. Alex Eng J. 2023;79:296–307.
[28] Az-Zo'Bi EA, Dawoud KA, Marashdeh M. Numeric-analytic solutions of mixed-type systems of balance laws. Appl Math Com. 2015;265:133–43.
[29] Rodgers L, Nicewander WA. Thirteen ways to look at the correlation coefficient. Am Stat. 1988;42(1):59–66.
[30] Zoubiri FZ, Rihani R, Bentahar F. Golden section algorithm to optimise the chemical pretreatment of agro-industrial waste for sugars extraction. Fuel. 2020;266:117028.
[31] Arnold W, Rottenkolber E, Hartmann T. DRAGON - The German thermo-chemical code based on the Becker-Kistiakowsky-Wilson equation of State. Propell Explos Pyrot. 2023;48:e202100329.